

# Effects of Curing on Emulsion Cold Mix Asphalts and Their Extracted Binder

**Amelie Thiriet** (✉ [amelie.thiriet@univ-eiffel.fr](mailto:amelie.thiriet@univ-eiffel.fr))

Université Gustave Eiffel - Campus de Nantes: Université Gustave Eiffel - Campus de Nantes  
<https://orcid.org/0000-0003-3223-2546>

**Vincent Gaudefroy**

Université Gustave Eiffel - Campus de Nantes: Université Gustave Eiffel - Campus de Nantes

**Emmanuel Chailleux**

Université Gustave Eiffel - Campus de Nantes: Université Gustave Eiffel - Campus de Nantes

**Jean-Michel Piau**

Université Gustave Eiffel - Campus de Nantes: Université Gustave Eiffel - Campus de Nantes

**Frédéric Delfosse**

Routes de France

**Christine Leroy**

Routes de France

---

## Research

**Keywords:** curing, emulsion cold mix asphalt, binder, oedometer test, rheology

**Posted Date:** December 7th, 2020

**DOI:** <https://doi.org/10.21203/rs.3.rs-119407/v1>

**License:**   This work is licensed under a Creative Commons Attribution 4.0 International License.

[Read Full License](#)

---

# Effects of curing on emulsion cold mix asphalts and their extracted binder

Amélie Thiriet<sup>1</sup>, Vincent Gaudefroy<sup>1\*</sup>, Emmanuel Chailleux<sup>1</sup>, Jean-Michel Piau<sup>1</sup>, Frédéric Delfosse<sup>2</sup>, Christine Leroy<sup>2</sup>

5 <sup>1</sup> Université Gustave Eiffel/IFSTTAR (French institute of science and technology for transport, development and network), Nantes, France

<sup>2</sup> Routes de France, Paris, France

\*Corresponding author: [vincent.gaudefroy@univ-eiffel.fr](mailto:vincent.gaudefroy@univ-eiffel.fr)

## 10 **Abstract**

This paper focuses on the physicochemical changes that happen in cold mix asphalts during curing, and more specifically, while and after transitioning to different simulated seasons. Several tests were carried out in order to better grasp the influence of the weather (temperature and humidity) on the curing of such materials. The mechanical behaviour of the mix was assessed using oedometer tests. The physicochemical evolutions of extracted binders, such as oxidation and rheology, were evaluated. The results show stiffening of the mix and ageing of the binder linked to a higher temperature and a lower humidity. A low temperature and high moisture seem to slow down these evolutions. However the binder behaviour does not explain the whole mix behaviour as the kinetics between them are not always similar. Thus other mechanisms are yet to be found and taken into account to fully understand cold mix asphalts behaviour.

15

20

**Keywords:** curing, emulsion cold mix asphalt, binder, oedometer test, rheology

## 1. Introduction

5 Cold mix asphalts are a composite material obtained by mixing a bitumen emulsion (bitumen droplets dispersed in an aqueous phase) with aggregates. At the final stage aggregates are linked together by the organic binder after the emulsion break. The material stiffens with time while water drains off in a phase called curing.

These materials are mostly used for pavement (road repair and structure of low traffic roads).  
10 This type of material could be an answer to the ecological issue. Contrary to hot mix asphalts which are manufactured at 160 °C, cold mix asphalts process requires emulsified bitumen and cold and wet rocks, saving energy to heat it up and preventing fumes generation. Nevertheless, cold mix mechanical behaviour during curing is relatively unknown and final performances are difficult to predict. The presence of water and its removal are one of the main differences  
15 compared to hot mix asphalt and they greatly influence the evolution of such a material. Furthermore it is known that the curing of emulsion cold mix asphalt is highly dependent on external parameters such as the climatic conditions [1, 2] or the composition [3]. Apart from increase of stiffness, the curing also influences other aspects of the material as stiffening and oxidation (ageing) of the binder, as is has already been studied for hot and cold bituminous  
20 mixes [4, 5, 6, 7].

To improve knowledge on emulsion cold mix asphalts and thus facilitate their use, an assessment of their behaviour during curing and a better understanding of their curing mechanisms are needed. The ambition of this paper is to give an idea of the different aspects of curing on emulsion cold mix asphalts and understand the influence of the implementation

season. These issues were assessed by comparing the mix mechanical evolution with the physicochemical characteristics of the binder with time. This comparison will give information about the different physical and chemical phenomena involved in the curing process. More precisely, cold mix asphalt samples were tested by oedometer test all along curing and their binder was extracted and studied at different curing times, with IR, rheology and calorimetry. The rheological evolution of the binder allows a direct understanding of the influence of the binder on the whole mix. A change in glass transition measured with calorimetry could account for binder weakening during curing. The oxidation (quantified with IR) and increase of modulus of the binder would indicate its ageing.

10

## **2. Materials and methods**

### **2.1 Materials**

The emulsion cold mix asphalt samples were made with a 70/100 bitumen emulsion at 65/35 bitumen-water ratio and virgin aggregates. The residual binder content was 4.55% and the total water content 6.50%. The material was compacted at 10% void content in cylindrical molds (120 mm diameter, 60 mm height).

15

### **2.2 Conditioning procedures**

All the samples were cured in a BIA CL1-30 climatic chamber at the following parameters:

20

- Three samples were cured at 35 °C and 20 % RH during two months followed by 10 °C and 80 %RH for two months. This group is called group A.
- Two samples went through two months at 10 °C and 80 %RH and then two months at 35 °C and 20 %RH. This group is called group B.

The 35 °C and 20 %RH curing parameters have been numerously applied in the literature [6, 7, 8, 10] in particular when used for 15 days to simulate two or three summers of curing on-site. In this study, they are used to simulate warm season. The 10 °C – 80 %RH parameters are chosen to simulate a cold season.

5        The samples were then removed from the chamber at specific times and separated into two testing groups: a batch of samples was tested with oedometric testing while the binder was extracted from samples of the other batch all along the curing process.

## 2.3 Test procedure

### 10    2.3.1 Oedometric tests

The mechanical behaviour of the samples was evaluated with a Schenck Prüfraahmen Typ press to measure the oedometric moduli at different curing times according to Lambert's method [9]. This technique uses cyclic compression of a specimen that is set in a cylindrical mold (120 mm diameter) to calculate the stiffness of a non-cohesive material. As the sample is contained in  
15    the mold, only vertical displacements occur. The determination of the modulus is calculated by dividing the stress amplitude with the strain amplitude from the stress-strain cycles obtained with oedometer testing.

Along with the oedometer tests, these samples were regularly weighed. Assuming that when the weight was minimal the samples were dry, the water content versus time was deduced with  
20    the equation  $100\% \times (m_{\text{sample}}(t) - m_{\text{sample}}(\text{min})) / (m_{\text{sample}}(t=0) - m_{\text{sample}}(\text{min}))$ .

### 2.3.2 Binder extraction procedure

The binder was extracted from the samples using an Asphalt Analysator and tetrachloroethylene as solvent. Prior to the extraction process, those samples were lyophilized with an Alpha 1-2 plate LDplus (Bioblock-Christ) freeze dryer in order to remove water, without using drying and heating steps to prevent further curing and oxidation. The collected binder was then centrifuged and distilled to remove the sand from the mix and the perchloroethylene from the extraction. After this procedure, the rheological behaviour, the glass transition and the oxidation of the extracted binders were studied.

### 2.3.3 Complex modulus measurement

The rheology measurements were done using an Anton Paar MCR102 DSR. Two plate-plate sample holders were used: an 8 mm diameter one for a range of temperature from 20 to -10 °C (5000 Pa imposed stress) and a 25 mm diameter one for a range from 20 to 80 °C (500 Pa imposed stress). Both ranges of temperatures were tested between 0.1 and 100 Hz.

### 2.3.4 DSC

Two different samples were tested in calorimetry for each extracted binder with a Mettler Toledo DSC3 DSC, the data was retrieved during an increase of temperature at 10 °C/min. The data given in the results section of this paper are the mean values between the two tests.

### 2.3.5 FTIR

Finally, the FTIR tests consisted in measuring the oxidation levels SO and CO of the binders by transmission on thin film, on five samples for each extracted binder. The device used was a Perkin Elmer Spectrum.

### 3. Results

#### 3.1 Evolution of the water content and samples geometry

5

Figure 1. Water content versus curing time in samples from group A (a) and B (b). Here we suppose that when the water content is minimal, the samples are dry. The following equation is used to calculate the relative water content at curing time  $t$ :  $100\% \times (m_{\text{sample}}(t) - m_{\text{sample}}(\text{min})) / (m_{\text{sample}}(t=0) - m_{\text{sample}}(\text{min}))$ .

10

Figure 1 shows the water contents in groups A and B. The kinetics of water loss is higher for group A (figure 1.-a): the samples are supposed dry after around 15 days, while samples from group B (figure 1.-b) are supposed dry after 70 days (beginning of the « summer » modality). Specimens from group A incorporate a small amount of water during the cold period (10 °C – 15 80 %RH) and specimens from group B experience a severe drying when going from cold to warm conditions.

Figure 2. Water content versus height of the samples from group A.

20 Figure 3. Heights of samples from group A (a) and B (b).

For group A (figure 2), there is a good correlation between water content and height: specimens loose height (around 1 mm) at the same time as water (during the 35 °C – 20 %RH modality, figure 3.-a) and gain height and water during the cold curing conditions.

Group B (figure 3.-b) behaviour is slightly different: during the cold period (the first 60 days), the specimens loose water (figure 1.-b) but their height remains constant (around 60.3 mm). Moreover, during the 35 °C – 20 %RH curing process, what was left of water in the samples is lost in about 7 days, while the shrinkage happens during more than a month (from about 71 to 108 curing days). Then, the height does not seem to change anymore. This could be explained by the rheological behaviour of the binder and the mix moisture during curing. The volume is mainly influenced by the binder movements. At 10 °C and 80 %RH the binder is less soft (around  $10^7$  Pa at 10 °C and 10 Hz) and there is still a high amount of water in the samples. This could prevent the mix shrinkage. After transition from 10 °C – 80 %RH to 35 °C and 20 %RH conditions, the binder is softer (around  $10^6$  Pa at 35 °C and 10 Hz) than at 10 °C so a shrinkage would be easier. The time difference between total loss of water (around 7 days) and the mix shrinkage (more than a month) can simply be explained by the high viscosity of the material resulting in a height loss inertia after water departure.

The height variations are also be correlated to the void geometry that would change during curing and influence the modulus of the material. As a matter of fact, the void percentage of every sample was measured at the end of curing and the void content with curing time was deduced from the variations of geometry of each sample (figure 4), with the hypothesis that no material had been lost during the whole curing and that the void content is proportional to the height. At the end of the 4 months of curing, group A lost between 0,13 and 0,24% voids and group B between 0,08 and 0,11%, which would imply a stiffening of both groups.

Figure 4. Void content versus curing time of group A (a) and B (b).

### 3.2 Rheological behaviour of the mixture

The stiffness modulus of the samples was assessed with an oedometer device [9]. Usually, other  
5 types of mechanical tests (indirect tensile or two-point bending for example) are used for the  
characterization of asphalt mixes as they are already very stiff at an early age. Asphalt cold  
mixes take time to cure and become more cohesive to be tested with these devices, they are  
very weak at young age. Therefore the oedometer test appears to be a suitable testing technique  
to measure their mechanical behaviour.

10

Figure 5. Mean stiffness evolution of groups A and B with time, tested at 15 °C, 10 Hz and 9.5  
kN. The error bars represent the standard deviation on the three samples for group A and two  
for group B.

15 Figure 5 displays the mean evolutions of oedometric modulus versus time for the samples  
from groups A and B (3 samples for group A and 2 for group B).

The kinetics of stiffness evolution are very different from one another. Indeed group A  
evolves rapidly and its modulus reaches more than 3000 MPa after 60 days, when the one from  
group B reaches a value of about 2300 MPa for the same period. The second curing conditions  
20 applied swap the temperature and moisture between the groups. The modulus of samples from  
group A remain constant while the modulus of group B increases. For both conditioning  
procedure, stiffness increases slowly during the cold period and more quickly during a warm  
period. Finally, the modulus values for both groups are similar at the end of the curing process,

which shows that seasons sequence does not influence the curing of the material after about 130 days throughout the modulus.

Figure 6. Mean stiffness evolution of groups A and B versus mean water content, modulus tested at 15 °C, 10 Hz and 9.5 kN. The error bars represent the standard deviation on the three samples for group A and two for group B. Once again, we suppose that when the water content is minimal, the samples are dry.

Moreover, these evolutions can be compared to the water content in the samples (fig. 6). Actually, in a general way, the modulus is lower when the water content is higher, and vice versa, when the water content is low, the modulus is higher. Besides the important stiffening at the beginning of curing for group A happens at the same time as the fast water loss of the samples (fig.1-a). In addition, the sudden increase of stiffness at the very beginning of the warm season for group B (around 70 days) can be correlated to the sharp decrease of water content at the same time (fig.1-b). But the presence of water does not explain the whole behaviour of the material as it continues to evolve even when the water content is stable [10].

A change in the void content could also be correlated to the height variations and therefore influence the modulus: a decrease in void content would lead to a decrease in height thus an increase in modulus; whereas an increase in void content would result in an increase in height and a decrease in modulus. For example such as seen in the 10 °C – 80 %RH period of group A where the change in height would counteract the stiffening than happens normally over time.

Additionally, the void content results mentioned above could only explain part of the stiffening as the final and initial states of samples from both groups A and B are similar while the void content variations are higher for group A than for group B.

5 Figure 7. Mean phase angle evolution of groups A and B with time, tested at 15 °C, 10 Hz and 9.5 kN. The error bars represent the standard deviation on the three samples for group A and two for group B.

10 The phase angle represents the delay between the stress and strain signals. Overall, the phase angle of both groups shown in figure 7 stays constant throughout the four months of curing. This indicates that the viscous behaviour of the material is not time dependent, regardless of the curing parameters. Moreover this data is in the same scale as can be found in the literature for cold mix asphalt [6].

### 15 3.3 Extracted binder evolution

As mentioned above, the comprehension of the physicochemical evolution of the binder could be extremely useful to grasp the whole mix behavior and better understand the mechanisms at play during the curing process. The rheology, glass temperature and oxidation bring  
20 information on the chemical variations and ageing of the binder.

#### 3.3.1 Rheological behaviour

##### 3.3.1.1 Shear modulus and phase angle

Figure 8. Magnitude of  $G^*$  with time, tested at 20 °C and 10 Hz. The error bars represent the standard deviation on the two tests (for two ranges of temperature, as explained in the test procedure concerning the rheology) performed for each point on each sample.

5

Figure 8 highlights the differences in stiffening kinetics induced by the two different curing conditions. The literature shows that the shear modulus of a binder extracted from on-site cold mix asphalt increases with time [8], which is consistent with our results since the modulus of both groups has increased in four months. The standard deviation between the two furthest  
10 initial ( $t=0$ ) points is used to decide whether the following points are significantly different or not. For each mean value, this standard deviation is subtracted or added in order to get an upper and lower limit. If the modulus value of a point at curing time  $t_n$  is included between the two limits of the previous point  $t_{n-1}$  then the studied point  $t_n$  is considered having a similar modulus value than the  $t_{n-1}$  point.

15 Group A exhibits a fast increase of the complex shear modulus during the 60 first days at 35 °C – 20 %RH and its stagnation during the next 60 days at 10 °C – 80 %RH as the modulus values at these curing conditions are considered similar.

As for group B, the shear modulus seems to slightly decrease with time during curing at 10 °C and 80 %RH as the first and last points of these curing conditions are considered  
20 significantly different. During curing at 35 °C – 20 %RH, the modulus then rises and reaches a value of about 7 MPa after 90 days in a similar way than the one for group A at the same curing conditions. This evolution would probably lead to the same final state for both groups.

Figure 9. Phase angle versus curing time, tested at 20 °C and 10 Hz. The error bars represent the standard deviation on the two tests performed throughout the curing process on each sample.

The significance of deviation between the phase angle points has been assessed the same way as previously on the shear modulus. The phase angle of the extracted binders of both groups does not highly evolve as it stays around 47-52° for group A and between 52 and 59° for group B (figure 9). The evolution of group A is overall considered not significant except for the three last points that are considered different from the initial one so the phase angle has slightly decreased. Moreover, concerning group B, the evolutions between beginning of curing and the points at 14 curing days and the final one are considered significantly different. Besides the other two points are also considered different from the initial one. This means that the phase angle of group B increases until around 60 days and then decreases. The lack of evolution of the phase angle during the 4 months of curing is concordant with the evolution observed on the asphalt mix. This was expected as the viscous behaviour of the material is largely, if only, influenced by the binder. However some light trends emerge, which may be more significant at longer curing times, such as a slight reduction during a 35 °C – 20 %RH period, and a small increase of the phase angle at 10 °C – 80 %RH.

### 3.3.1.2 Representation in the Black space

20

Figure 10. Black diagram of the extracted binders of group A, a) Each colour represents a different extracted binder sample, b) Simplified zoom on results of tests at 20 °C and 10 Hz. The smaller blue points represent the extracted binder at t=0 and every tested temperatures and frequencies. Points 1 to 6 display respectively 0, 15, 30, 62, 91 and 120 days of curing. Points

1, 2, 3 and 4 correspond to 35 °C – 20 %RH while points 5 and 6 correspond to 10 °C – 80 %RH.

The Black diagram of group A is illustrated in figure 10. Points 1, 2, 3 and 4 concerning binders which curing was stopped at 0, 15, 30 and 62 days respectively, during the warm period, show a stiffening and a decrease of phase angle with time. A stiffening is consistent with the literature and [11] showed that this progression is consistent with a physical hardening. The last two points (5 and 6, 91 and 120 days of curing, 10 °C – 80 %RH) indicate a stagnation of the binder. Thus a cold period appears to hinder the stiffening of a binder, in cold mix asphalts.

10

Figure 11. Black diagram of the extracted binders of group B, a) Each colour represents a different extracted binder sample, b) Simplified zoom on results of tests at 20 °C and 10 Hz. The smaller blue points represent the extracted binder at t=0 and every tested temperatures and frequencies. Points 1 to 5 display respectively 0, 14, 29, 59 and 93 days of curing. Points 1, 2, 3 and 4 correspond to 10 °C – 80 %RH while point 5 corresponds to 35 °C – 20 %RH.

15

The series of the first 4 points (0, 14, 29 and 59 curing days at 10 °C – 80 %RH) on figure 11 show an even more significant trend to the one seen on figure 10 for the same simulated season: during the 2 months at 10 °C and 80 %RH, group A has lost half the stiffness that B has, and B has gained in phase angle where A has not. This difference in kinetics between A and B during cold conditions may be related to their initial states : group A has already been through a warmer period which may have started physicochemical processes that B has not seen yet, which would explain the inertia of softening seen on figure 10 between points 4 and 5. Then, after the transition to 35 °C – 20 %RH for group B (point 5), the binder gets even stiffer

20

and elastic than its initial state, which implies a certain reversibility in the mechanisms which occur during a cold period.

It is important to keep in mind that here the curing is only of 4 months in a climatic chamber this is why the data changes are very low. What is interesting is to extrapolate those results to longer curing times, where the changes would be far more significant, but the trends would probably remain the same.

### 3.3.2 Glass temperature and oxidation levels

Figure 12. Glass transition versus time of the extracted binders samples. The errors bars represent the standard deviation between the two DSC results.

The glass transition (figure 12) does not significantly change during the whole curing process.

Infra-red oxidation levels were measured on the extracted binders of the samples from groups A and B. Figure 13 shows the carbonyl (figure 13-a) and sulfoxide (figure 13-b) oxidation indexes of these specimens at different curing times.

Figure 13. Carbonyl (a) and Sulfoxide (b) oxidations indexes of the binders extracted at different curing times. The error bars represent the standard deviation of the five tests for each sample.

The initial and final oxidation levels of both groups A and B are equivalent. Moreover the kinetics of oxidation for both groups at warm period are similar as well as the ones during cold

period. During warm period (35 °C – 20 %RH, first two months of group A and last two months of group B), the carbonyl and sulfoxide oxidation indexes significantly increase with time. During cold period (10 °C – 80 %RH, last two months of group A and first two months of group B) they tend to be constant which shows that there seems to be no oxidation mechanism during a cold weather. These results show the effect of a temperature of 35 °C, that accelerates oxidation.

The increase of stiffness and oxidation during curing, especially during 35 °C – 20 %RH shows an oxidation of the binder. Colder conditions (10 °C – 80 %RH) seem to slow down this evolution.

10

#### **4. Discussion: Comparison between the mix mechanical behaviour and the physicochemical evolution of the extracted binder**

The  $\frac{\text{final modulus}}{\text{initial modulus}}$  coefficients are presented in Table 1 and 2. These coefficients can help to understand at what amount the stiffness increased : if the coefficient is close to 1, then the modulus did not evolve significantly ; if the coefficient is lower than 0, the modulus decreased with time ; finally if the coefficient is higher than 1 then the stiffness improved.

Table 1 represents the coefficients between the final and the initial shear modulus and Table 2 the same coefficients on the oedometric modulus, for each group and each modality, tested at 15 °C and 10 Hz. The 15 °C data for the extracted binder were extrapolated from the curves of  $|G^*|$  versus test temperature to allow an easy comparison between the mix and the binder data.

Table 1: Final/initial state coefficients of the extracted binder, calculated for 15 °C, and 10 Hz.

$ G^* $	Group A	Group B
Total curing process	1.41	1.16
First curing parameters	1.48	0.62
Second curing parameters	0.95	1.87

The first modality for group A corresponds to 35 °C – 20 %RH and for B 10 °C – 80 %RH.

The second one corresponds to 10 °C – 80 %RH for group A and 35 °C – 20 %RH for group B.

- 5 Table 2: Final/initial state coefficients of the emulsion cold mix asphalt (15 °C, 10 Hz and 9.5 kN).

$ E^* $	Group A	Group B
Total curing process	1.96	2.88
First curing parameters	1.80	2.02
Second curing parameters	1.09	1.43

The first modality for group A corresponds to 35 °C – 20 %RH and for B 10 °C – 80 %RH.

The second one corresponds to 10 °C – 80 %RH for group A and 35 °C – 20 %RH for group B.

10

First of all, the binder coefficients for each modality (Table 1) are quite close: at 35 °C and 20 %RH group A coefficient (first modality) reach around 1.5 and group B coefficient (second modality) around 1.9 which can be judged as similar. The same behaviour is noted for 10 °C and 80 %RH (second modality for group A and first one for group B) where the coefficients are both under 1, which means that the stiffness has slightly lowered with time (results consistent with the ones discussed in the Black planes part).

15

However, the results concerning the asphalt mix (Table 2) are mildly different as the total (« Total curing process ») and the 10 °C – 80 %RH coefficient of group B are a bit higher than the data from group A. More precisely, during the first modality (10 °C – 80 %RH) the stiffness of group B increases as much as the stiffness of group A (around 2 for both groups) whereas throughout the second modality, the coefficients of group B are a bit higher than the one of group A. This shows that different phenomena are at stake depending on the curing parameters: when the first modality is a cold one (10 °C – 80 %RH), not every curing physicochemical processes are triggered, which results in a continuation of stiffening after transition to the warm modality (35 °C – 20 %RH). On the contrary when the first modality is a warm one, the majority of the curing processes are induced, that is why the stiffening coefficients of the cold season as second modality are close to 1.

Finally the coefficients for each modality are reasonably close between the binder and the mix except for the first modality of group B: the mix coefficient reach 2 whereas the binder coefficient only 0.6. This indicates that the binder evolution only is not enough to justify the mix evolution: other phenomena come into play. A hypothesis could deal with the bitumen-aggregate contacts quality or the void geometry under the influence of water.

Concerning this part, it is important to keep in mind that these coefficients may also slightly differ with the curing time chosen for the calculations. For instance the very initial state (curing time = 0) of the mixes are not known as the oedometer tests have begun at 3 days of curing, this may explain the proximity in coefficients between both groups for the first modality ; if the initial time was 0, the coefficients of A would be higher than for B. Moreover there is no oedometer data between 49 and 71 days for group A so its coefficients may be fairly underestimated.

## 5. Conclusion

This paper has the purpose of bringing some new data concerning emulsion cold mix asphalts, giving leads and distinguishing the main phenomena influencing curing, and showing that it is often interesting to compare different scales of the studied material to understand its behaviour as much as possible.

The main results are :

- (1) The thickness of the samples varies with the water content which can influence the stiffness,
- (2) Regardless of the simulated season sequence inside the climatic chamber, based on isothermal curing processes at 35 °C or 10 °C, the final states of the samples are similar for both groups,
- (3) Warm and dry temperature-moisture parameters increase the stiffness of the material and its binder ageing,
- (4) Cold temperature and high moisture parameters result most of the time in a stagnation of the stiffness moduli (mix and binder) and oxidation,
- (5) The Black representation is an efficient way of comparing different curing conditions, in our case 35 °C – 20 %RH and 10 °C – 80 %RH,
- (6) The binder evolution does not entirely explain the mix evolution. Other physicochemical processes are to be taken into account to completely fathom this type of materials, such as the influence of water or the void geometry.

These materials appear to be an attractive way towards a more reasoned use of bitumen as less bitumen is required to implement them. Contrary to hot mix asphalts, their behaviour progresses with time and more research could be done to improve their optimal performances.

For example, the bitumen-aggregate contact mechanisms seem to take a non negligible part in curing depending on the water movements.

## **Declarations**

### 5 Availability of data and materials:

The dataset analysed during the current study are available from the corresponding author on reasonable request.

### Competing interests:

The authors declare that they have no competing interests.

### 10 Funding:

Not applicable.

### Authors' contributions:

AT took part in the acquisition and analysis of the oedometric data, performed and analysed all of the other tests and was a major contributor in writing the manuscript. VG and EC directed the study and helped on the interpretation of the extracted binder data. J-MP took a priceless part in the oedometer tests analysis and interpretation. FD and CL substantively revised this paper. All authors read and approved the final manuscript.

### Acknowledgements:

The authors acknowledge Jean-Luc Geffard for his considerable contribution concerning the oedometer tests.

## References

- [1] T. A. Doyle, C. McNally, A. Gibney and A. Tabaković, Developing maturity methods for the assessment of cold-mix bituminous materials. *Construction and Building Materials*. 38, 524-529 (2013).
- [2] C. K. Kumar, D. S. N. V. A. Kumar, M. A. Reddy and K. S. Reddy, Investigation of cold-in-place recycled mixes in India. *International Journal of Pavement Engineering*. 9, 265-274 (2008).
- [3] J.-P. Serfass, J.-E. Poirier, J.-P. Henrat and X. Carbonneau, Influence of curing on cold mix mechanical performance. *Materials and Structures*. 37, 365-368 (2004).
- [4] L. D. Poulikakos, B. Hofko, L. Porot, X. Lu, H. Fischer and N. Kringos, Impact of temperature on short– and long-term aging of asphalt binders. *RILEM Technical Letters*. 1, 6-9 (2016).
- [5] J. Lamontagne, P. Dumas, V. Mouillet and J. Kister, Comparison by Fourier transform infrared (FTIR) spectroscopy of different ageing techniques : application to road bitumens. *Fuel*. 80, 483-488 (2001).
- [6] A. Béghin, L. Wendling, X. Carbonneau, C. d. L. Roche, F. Delfosse, V. Gaudefroy, L. Odie, J.-M. Piau and J.-P. Triquigneaux, Behavior and design of grave-emulsion, public-private cooperation : Curing and evolution over time of the mix properties and binder characteristics. *European roads review (RGRA)*. 19, (2011).
- [7] J.-P. Triquigneaux, L. Wendling, L. Odie, D. Claudel and V. Gaudefroy, Behavior and study of emulsified asphalt mixes, public-private cooperation : Duriez test : voids content,

mechanical performance, sensitivity to water and characterization of extracted binders. European roads review (RGRA). 19, (2011).

[8] F. Delfosse, A. Béghin, A. Belkahia, V. Gaudefroy, C. Gueit and L. Odie, Comportement et étude des graves-émulsion, corrélation entre le comportement en place sur la RD 26 et le laboratoire. European roads review (RGRA, in French). 954, (2018).

[9] M. Lambert, J.-M. Piau, V. Gaudefroy, A. Millien, F. Dubois, C. Petit and F. Chaignon, Modeling of cold mix asphalt evolutive behaviour based on nonlinear viscoelastic spectral decomposition. Construction and Building Materials. 173, 403-410 (2018).

[10] J.-P. Serfass, X. Carbonneau, F. Delfosse and J.-P. Triquigneaux, Grave-emulsion assessment and behavior. RGRA. 889, (2010).

[11] G. Gauthier, D. Bodin, E. Chailleux and T. Gallet, Non Linearity in Bituminous Materials during Cyclic Tests. Road Materials and Pavement Design. 11, 379-410 (2010). doi.org/10.1080/14680629.2010.9690339.

# Figures

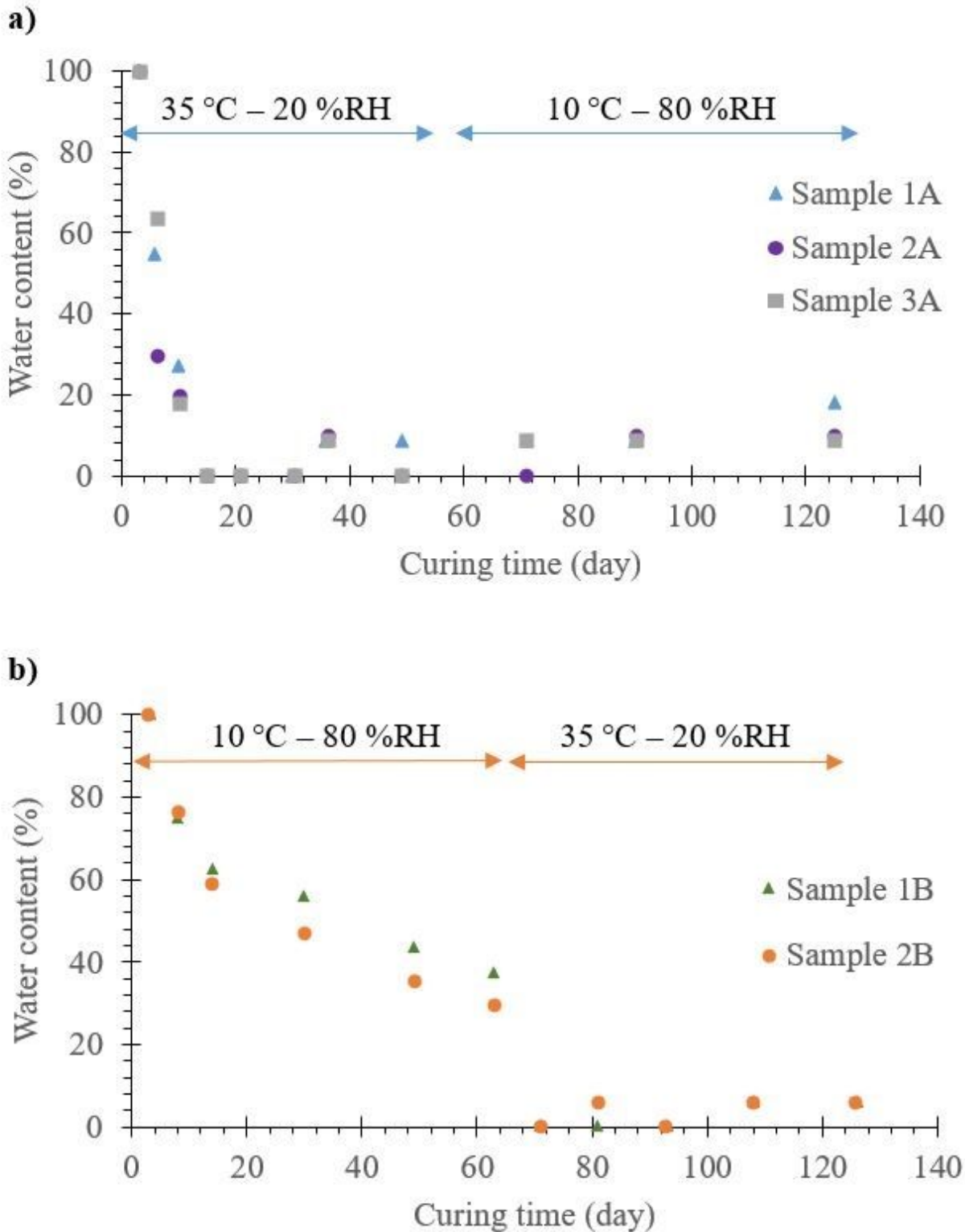


**Figure 1**

Water content versus curing time in samples from group A (a) and B (b). Here we suppose that when the water content is minimal, the samples are dry. The following equation is used to calculate the relative water content at curing time  $t$ :  $100\% \times (m_{\text{sample}}(t) - m_{\text{sample}}(\text{min})) / (m_{\text{sample}}(t=0) - m_{\text{sample}}(\text{min}))$ .

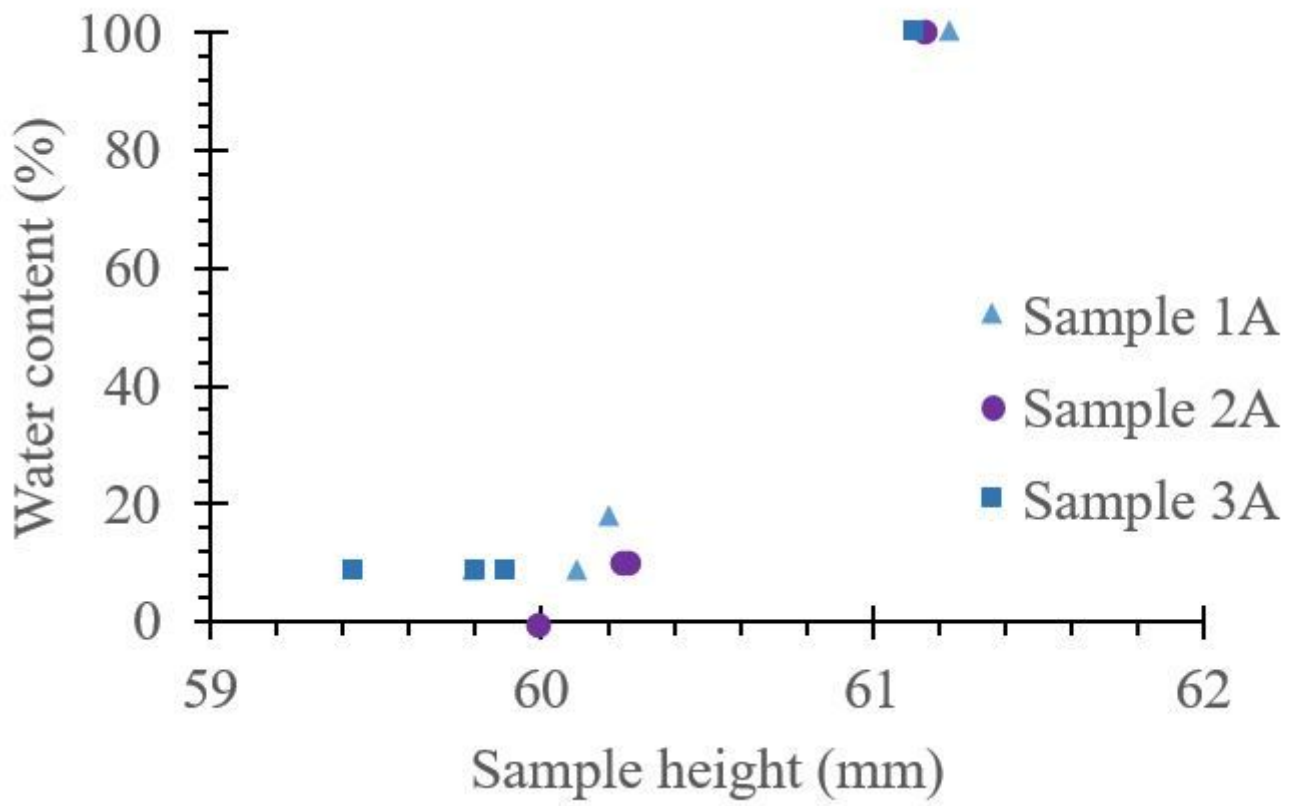
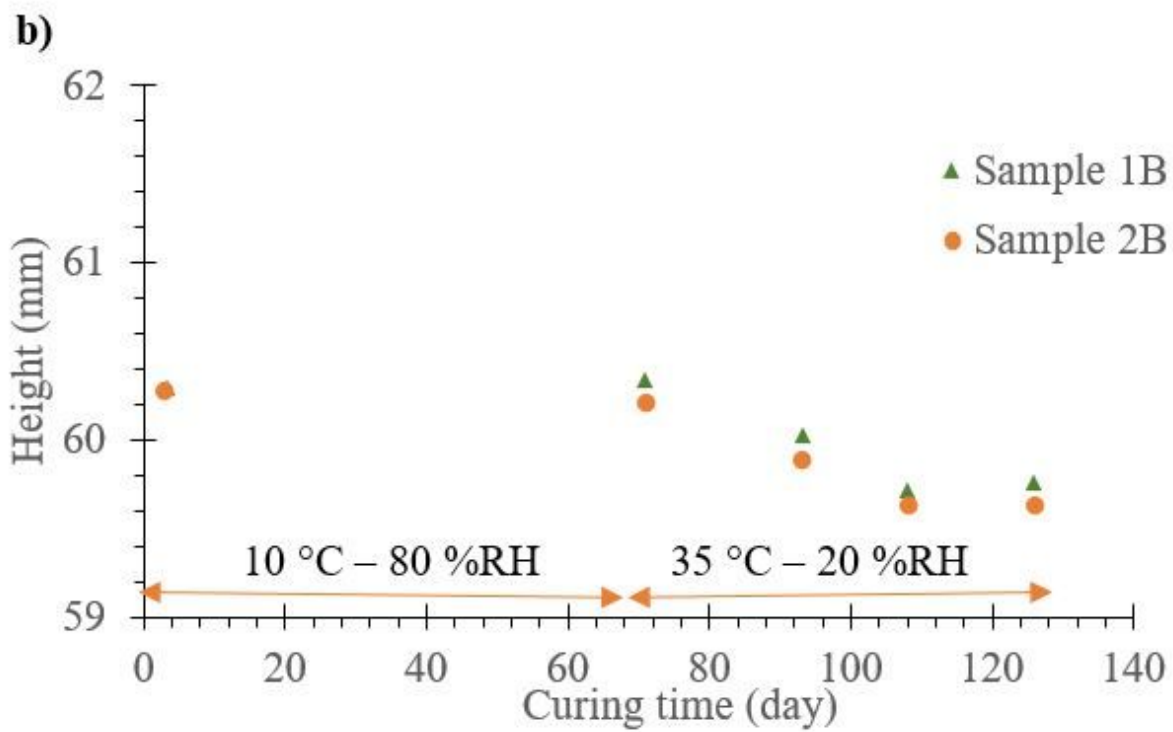
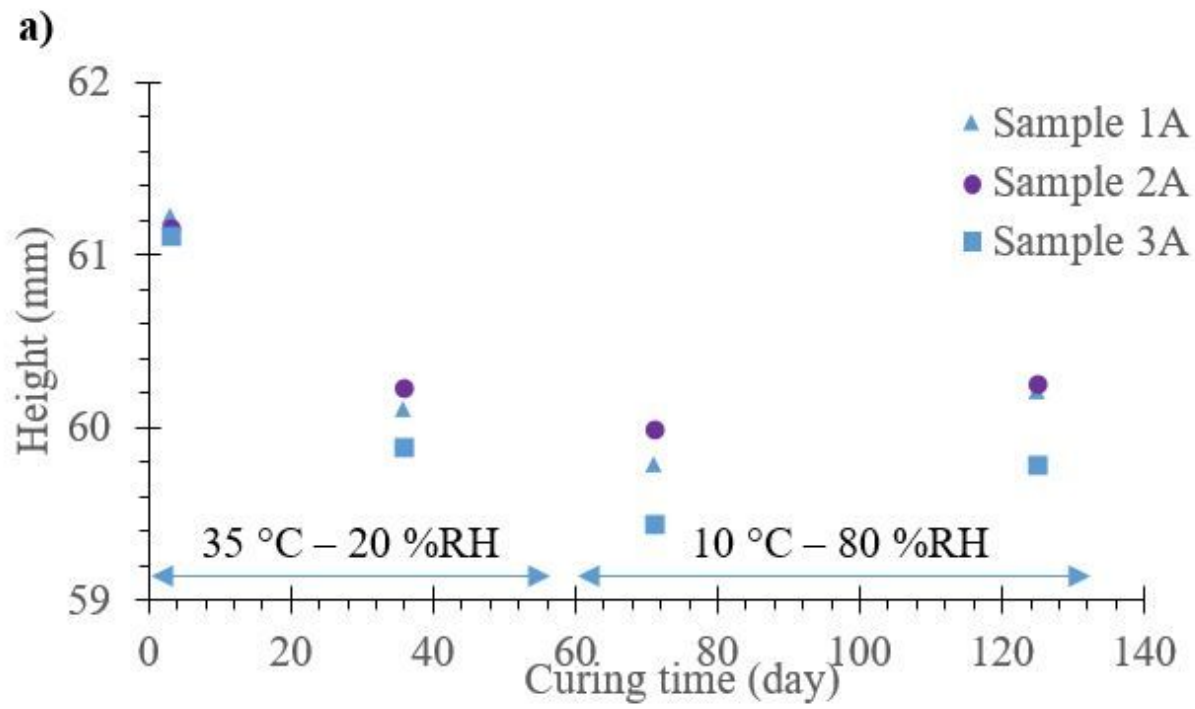


Figure 2

Water content versus height of the samples from group A.



**Figure 3**

Heights of samples from group A (a) and B (b).

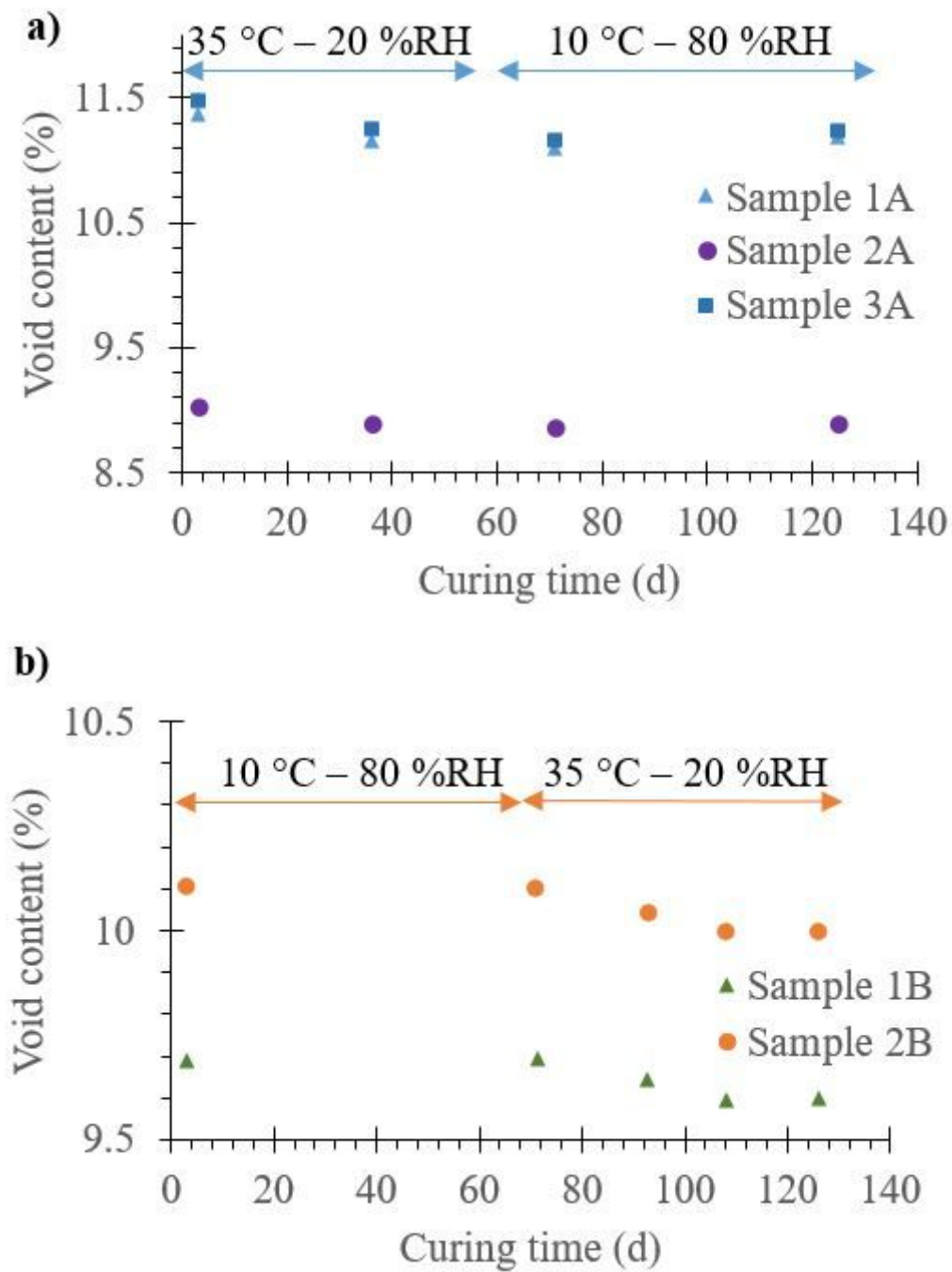


**Figure 4**

Void content versus curing time of group A (a) and B (b).

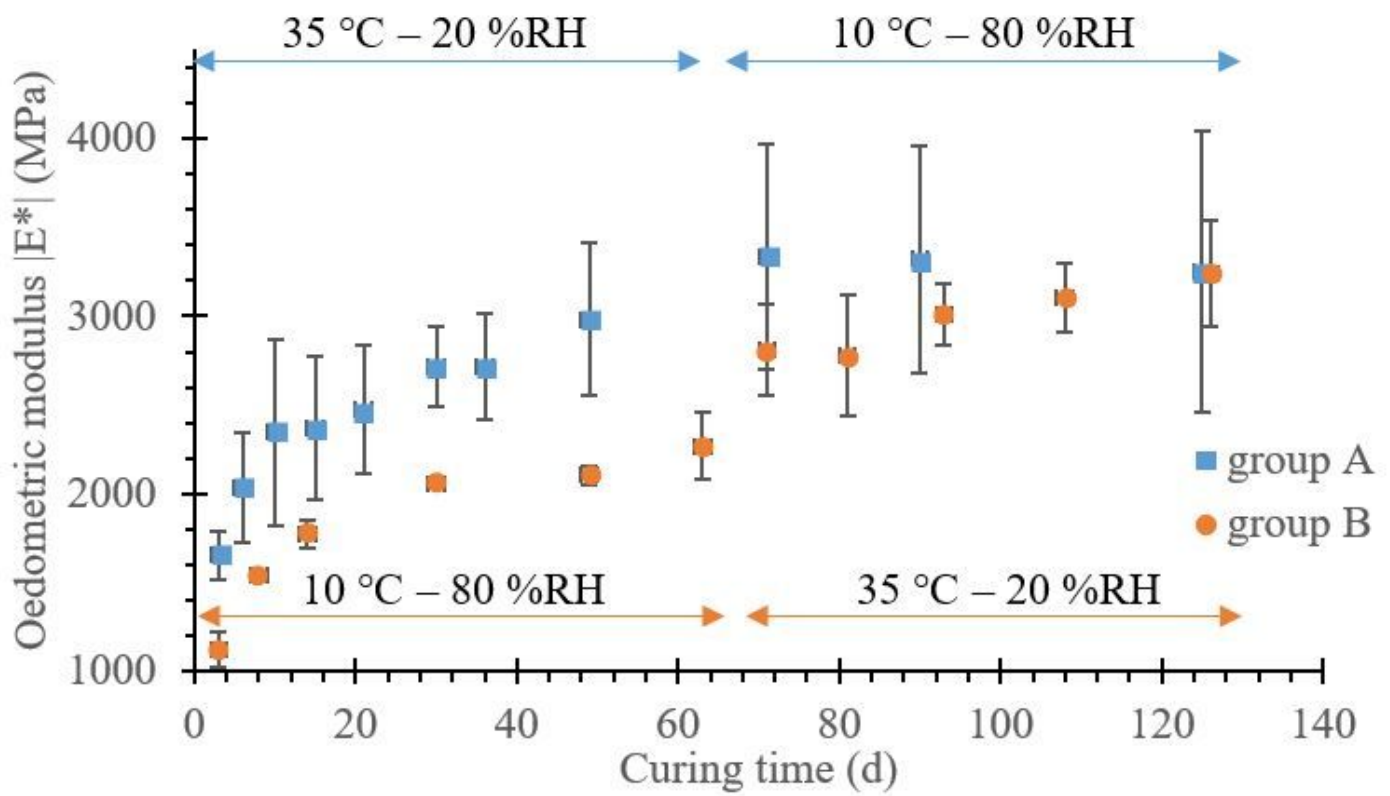


**Figure 5**

Mean stiffness evolution of groups A and B with time, tested at 15 °C, 10 Hz and 9.5 kN. The error bars represent the standard deviation on the three samples for group A and two for group B.

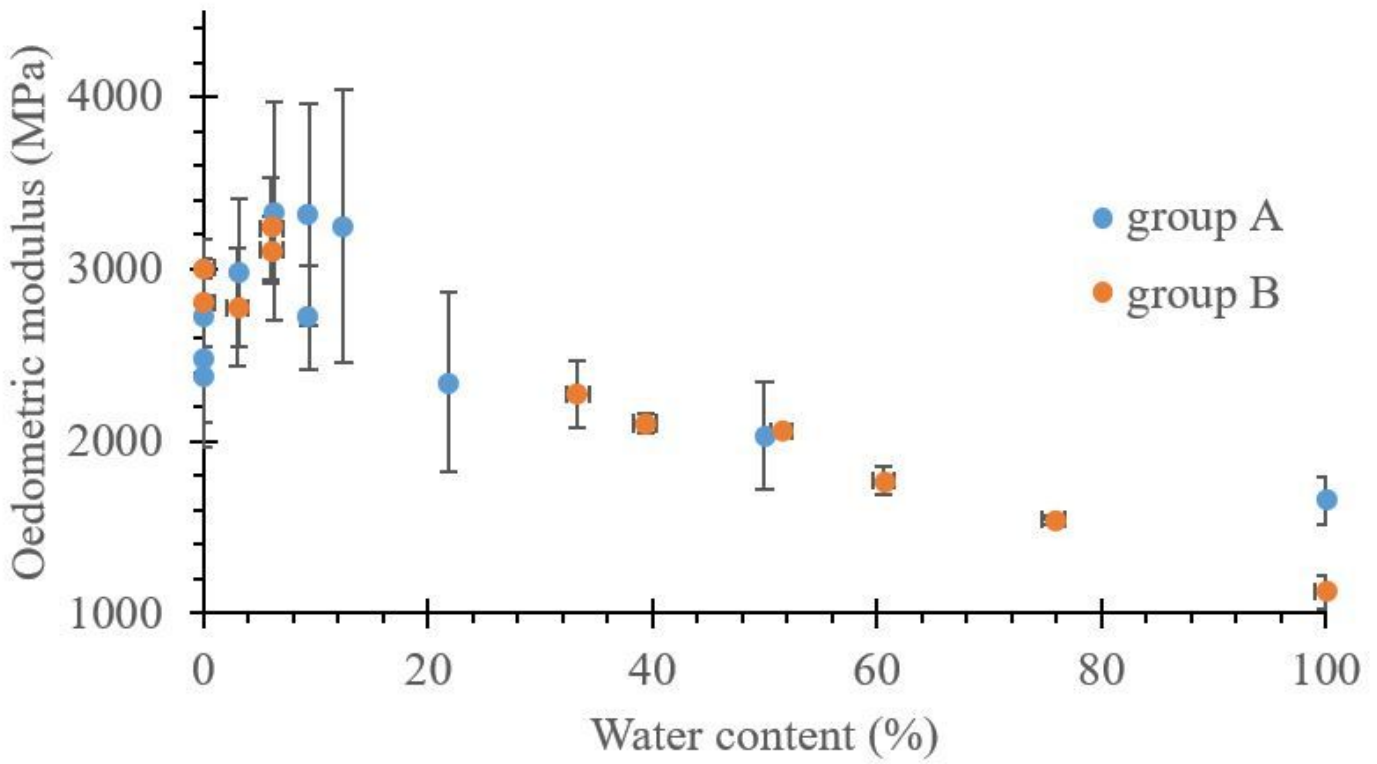


**Figure 6**

Mean stiffness evolution of groups A and B versus mean water content, modulus tested at 15 °C, 10 Hz and 9.5 kN. The error bars represent the standard deviation on the three samples for group A and two for group B. Once again, we suppose that when the water content is minimal, the samples are dry.

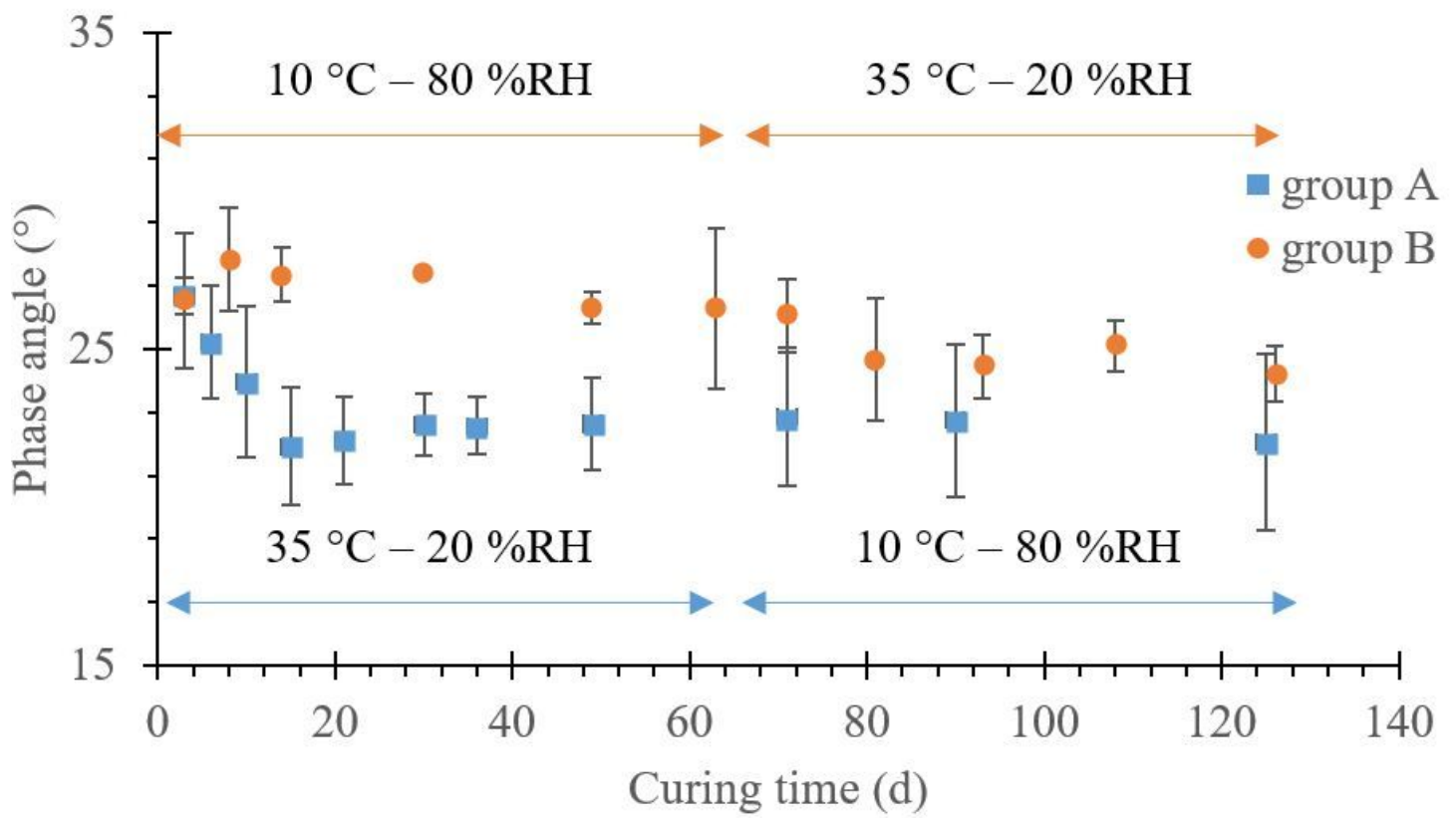


**Figure 7**

Mean phase angle evolution of groups A and B with time, tested at 15 °C, 10 Hz and 9.5 kN. The error bars represent the standard deviation on the three samples for group A and two for group B.

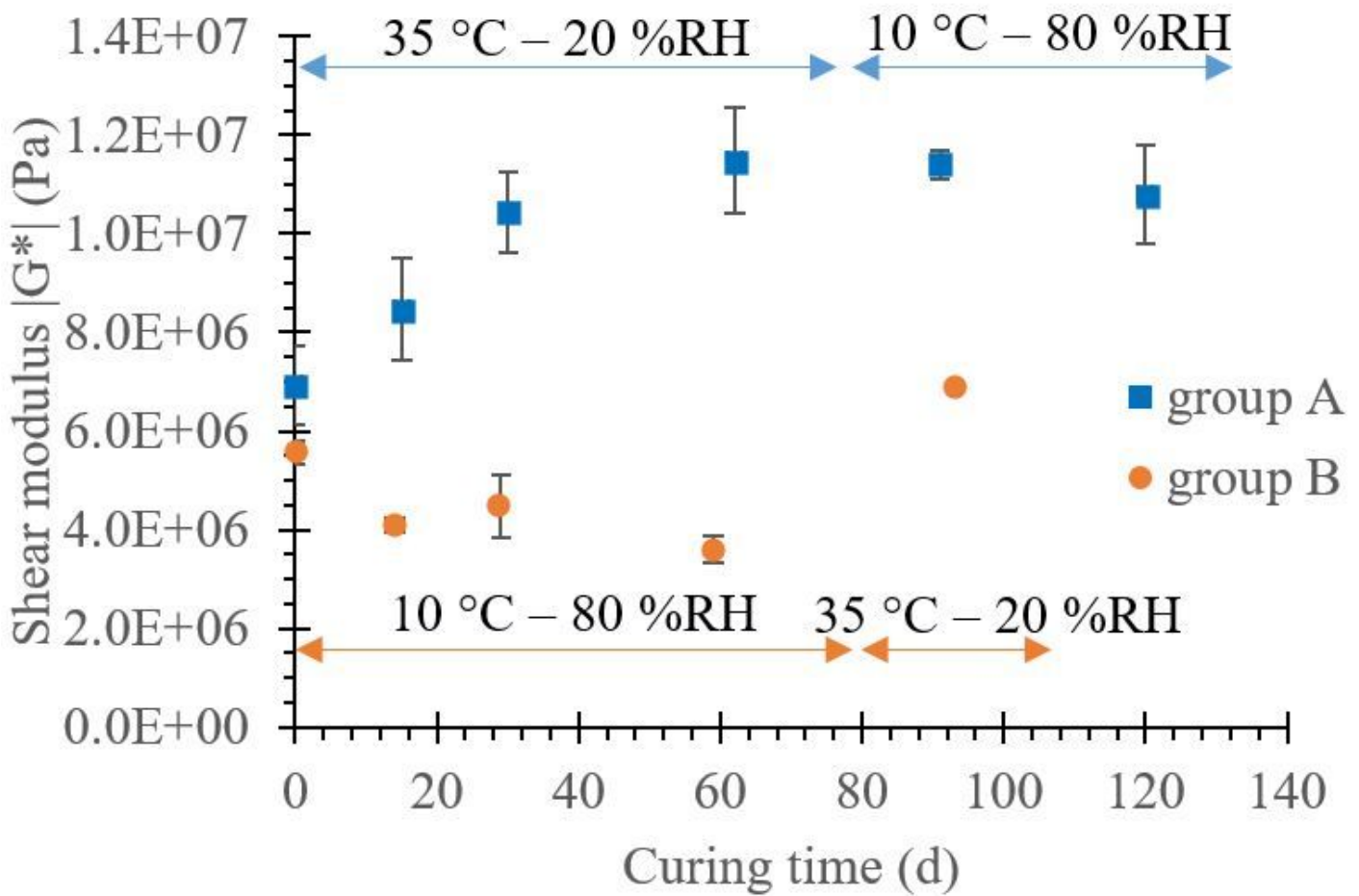


**Figure 8**

highlights the differences in stiffening kinetics induced by the two different curing conditions. The literature shows that the shear modulus of a binder extracted from on-site cold mix asphalt increases with time [8], which is consistent with our results since the modulus of both groups has increased in four months. The standard deviation between the two furthest initial ( $t=0$ ) points is used to decide whether the following points are significantly different or not. For each mean value, this standard deviation is subtracted or added in order to get an upper and lower limit. If the modulus value of a point at curing time  $t_n$  is included between the two limits of the previous point  $t_{n-1}$  then the studied point  $t_n$  is considered having a similar modulus value than the  $t_{n-1}$  point.

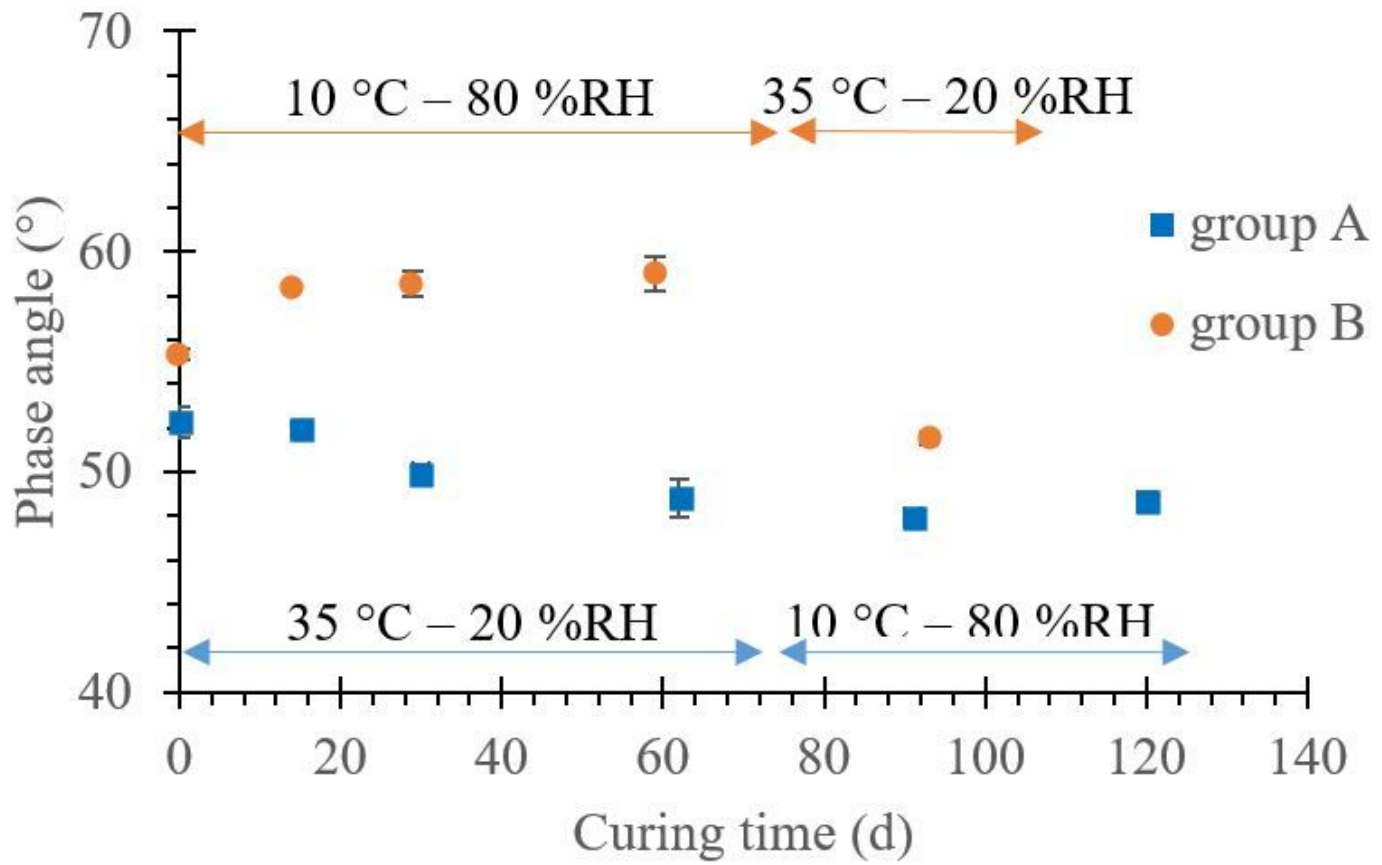


**Figure 9**

Phase angle versus curing time, tested at 20 °C and 10 Hz. The error bars represent the standard deviation on the two tests performed throughout the curing process on each sample.

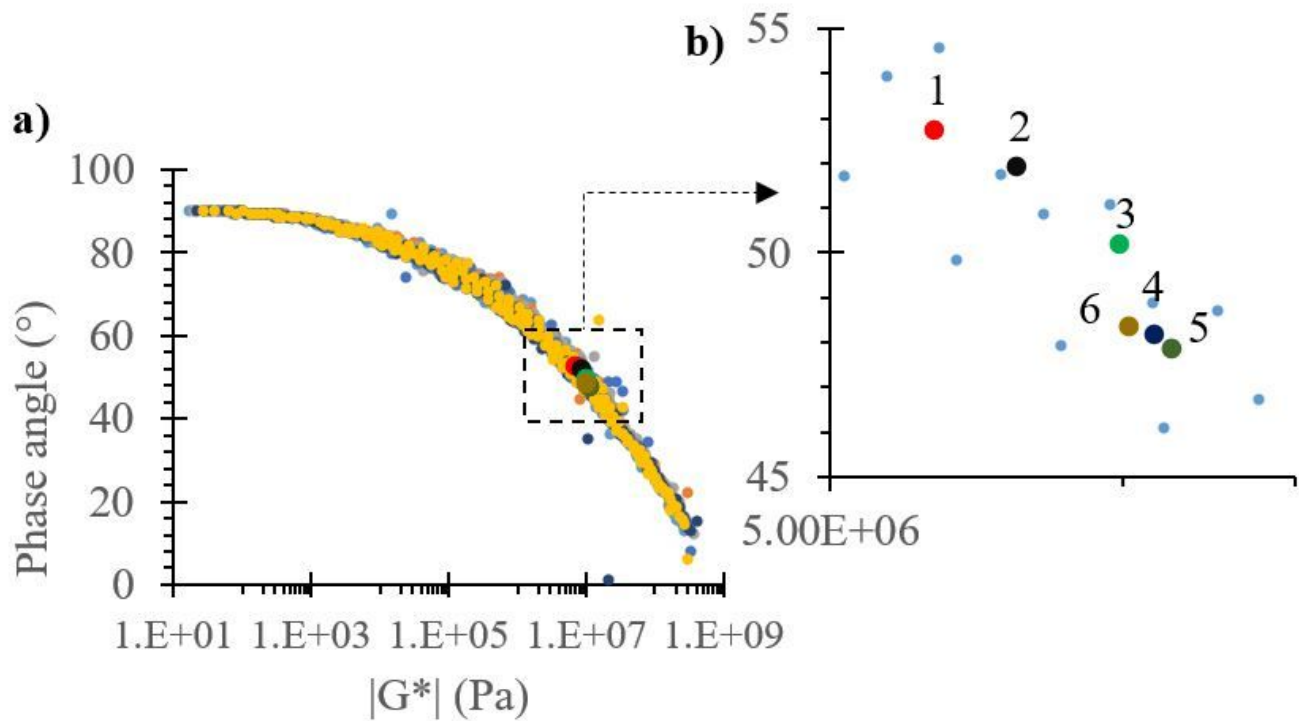


**Figure 10**

Black diagram of the extracted binders of group A, a) Each colour represents a different extracted binder sample, b) Simplified zoom on results of tests at 20 °C and 10 Hz. The smaller blue points represent the extracted binder at  $t=0$  and every tested temperatures and frequencies. Points 1 to 6 display respectively 0, 15, 30, 62, 91 and 120 days of curing. Points 1, 2, 3 and 4 correspond to 35 °C – 20 %RH while points 5 and 6 correspond to 10 °C – 80 %RH.

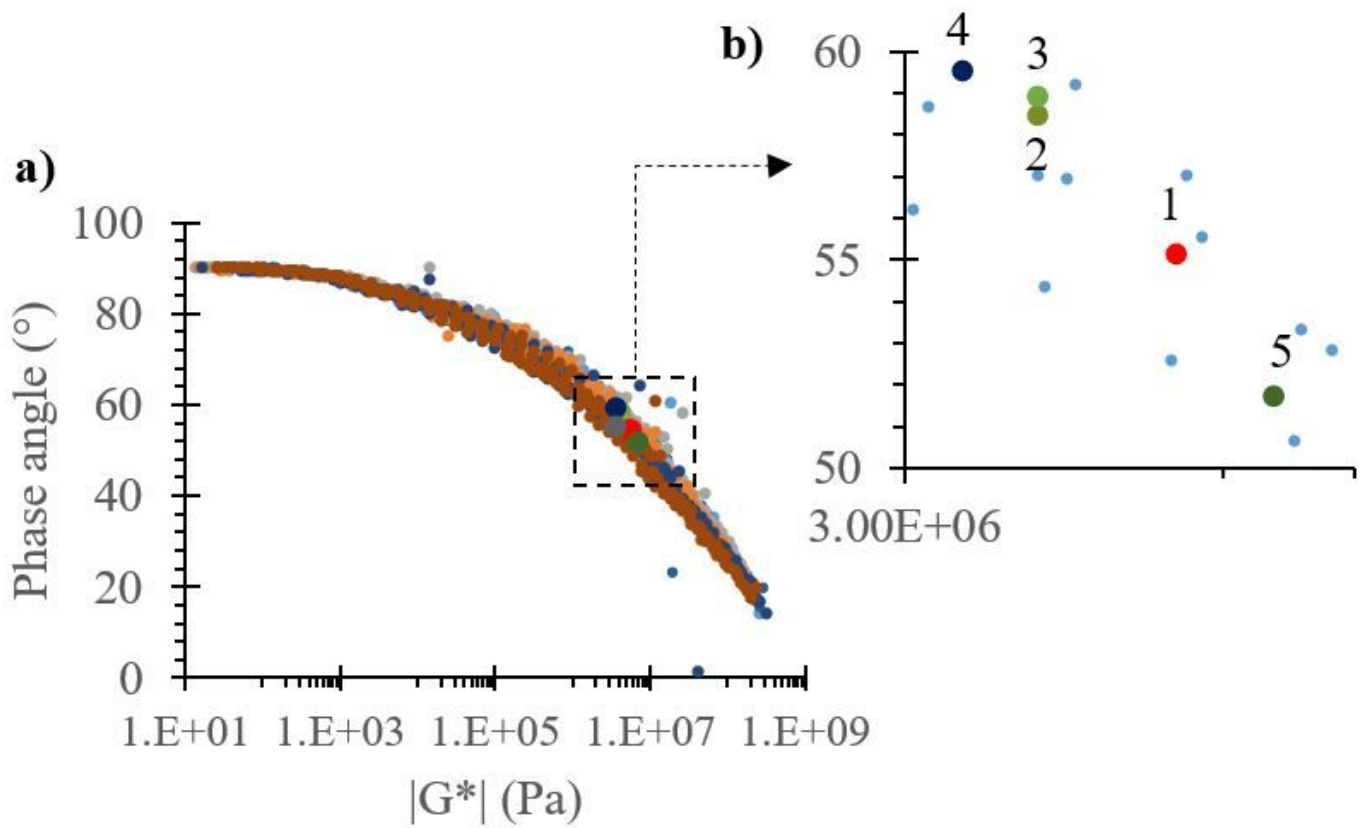


**Figure 11**

Black diagram of the extracted binders of group B, a) Each colour represents a different extracted binder sample, b) Simplified zoom on results of tests at 20 °C and 10 Hz. The smaller blue points represent the extracted binder at  $t=0$  and every tested temperatures and frequencies. Points 1 to 5 display respectively 0, 14, 29, 59 and 93 days of curing. Points 1, 2, 3 and 4 correspond to 10 °C – 80 %RH while point 5 corresponds to 35 °C – 20 %RH.

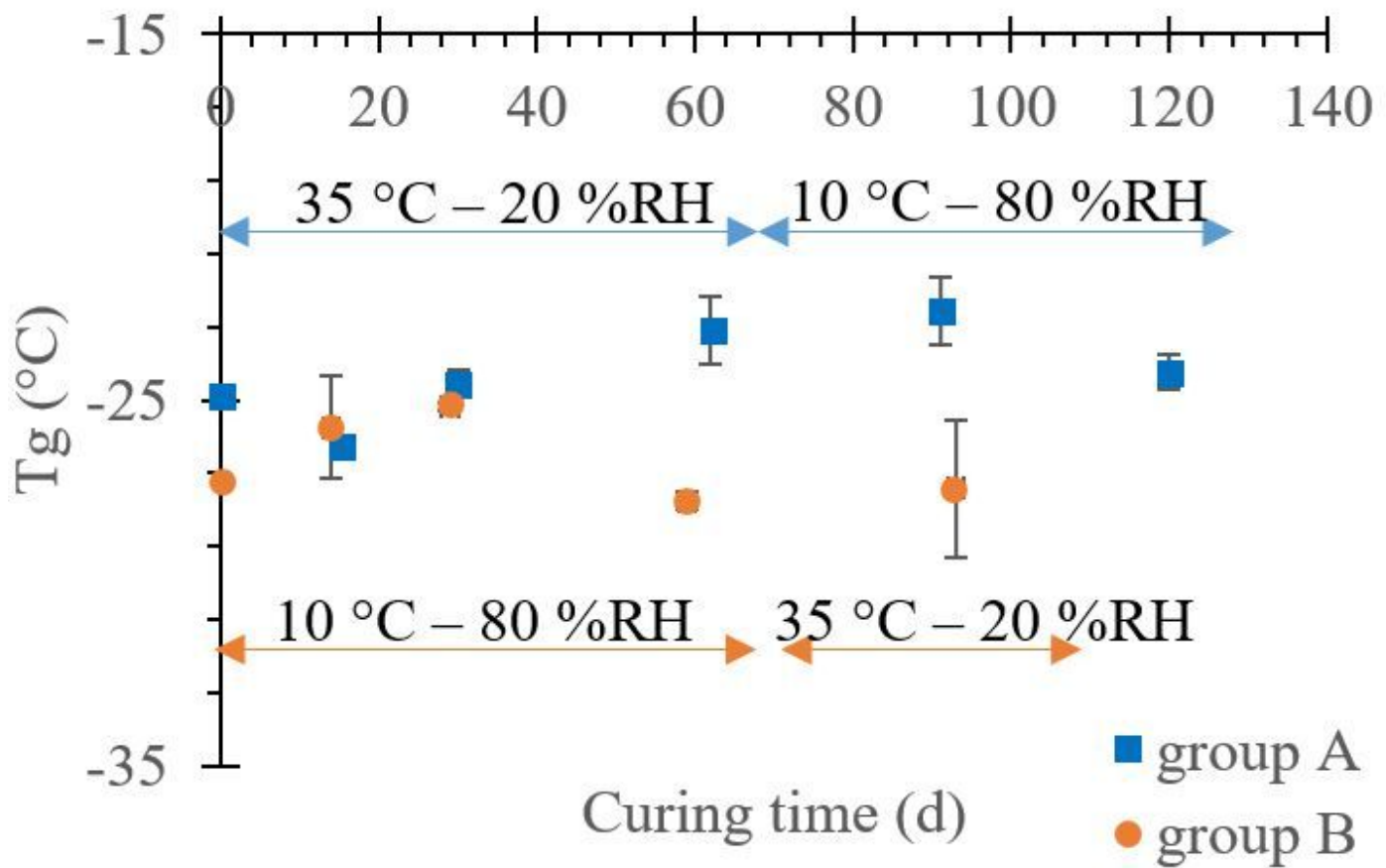
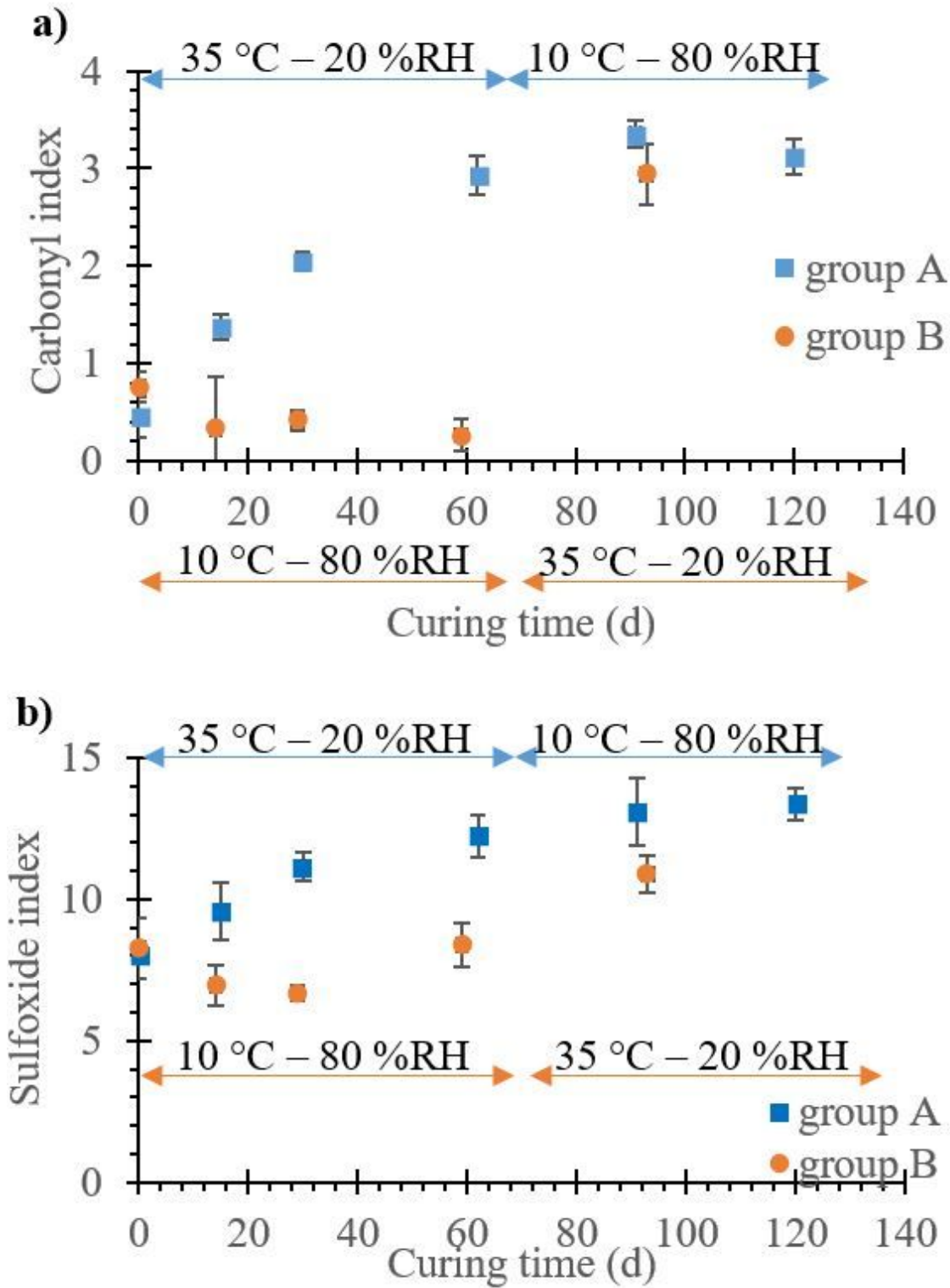


Figure 12

Glass transition versus time of the extracted binders samples. The errors bars represent the standard deviation between the two DSC results.



**Figure 13**

Carbonyl (a) and Sulfoxide (b) oxidations indexes of the binders extracted at different curing times. The error bars represent the standard deviation of the five tests for each sample.